2017 International Conference on Indoor Positioning and Indoor Navigation (IPIN), 18-21 September 2017, Sapporo, Japan

On-The-Fly Geometric Calibration of Inertial Sensor Arrays

Håkan Carlsson*, Isaac Skog* and Joakim Jaldén*
*Department of Information Science and Engineering, KTH Royal Institute of Technology, Stockholm, Sweden
(e-mail: hakcar@kth.se, skog@kth.se, jalden@kth.se)

***Abstract*—We present a maximum likelihood estimator for estimating the positions of accelerometers in an inertial sensor array. This method simultaneously estimates the positions of the accelerometers and the motion dynamics of the inertial sensor array and, therefore, does not require a predefined motion sequence nor any external equipment. Using an iterative block coordinate descent optimization strategy, the calibration problem can be solved with a complexity that is linear in the number of time samples.**

The proposed method is evaluated by Monte-Carlo simulations of an inertial sensor array built out of 32 inertial measurement units. The simulation results show that, if the array experiences sufficient dynamics, the position error is inversely proportional to the number of time samples used in the calibration sequence. Further, results show that for the considered array geometry and motion dynamics in the order of $2000^\circ\,/\mathrm{s}$ and $2000^\circ/\mathrm{s}^2$, the positions of the accelerometers can be estimated with an accuracy in the order of $10^{-6}\,\mathrm{m}$ using only 1000 time samples. This enables fast on-the-fly calibration of the geometric errors in an inertial sensor array by simply twisting it by hand for a few seconds.

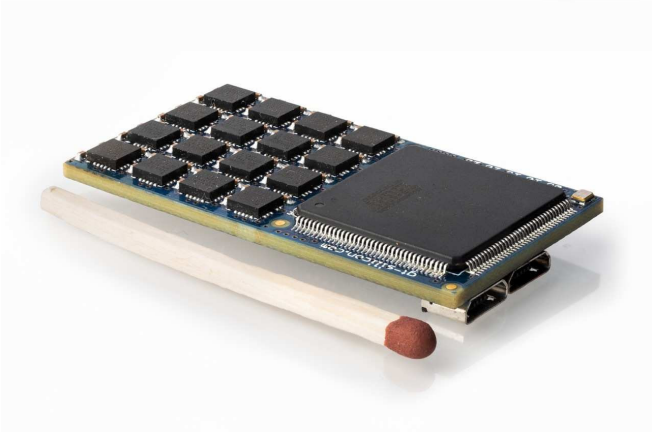

Fig. 1: In-house developed inertial sensor array with 288 sensing elements. The array is built out of 32 InvenSense MPU9150 sensor chips.

I. Introduction

Today, thanks to the development of micro-electro-mechanical-systems (MEMS) technology, miniaturized accelerometers, gyroscopes, and magnetometers can be produced at unprecedented volumes and at low prices [1]. Unfortunately, the performance of these ultra-low-cost sensors is too poor to enable reliable localization in many applications [2], [3]. However, by capitalizing on the small size, low price, and low power consumption of the sensors, it is now feasible to construct arrays with hundreds of sensing elements and fuse their measurements to create "super sensors" with high performance-to-price ratios; an example of a sensor array with 288 sensing elements is shown in Fig. 1.

A requirement for these "super sensors" to reach their full potential and achieve the theoretical performance presented in [4], is that the spatial geometry between the sensors is known with high accuracy; especially uncertainties in the geometry of the accelerometers could degrade the fusion of the measurements. Uncertainties in the positions of the accelerometers are caused by imperfections in the mounting of the sensors and lack of knowledge about the physical location of the sensing elements within the sensor chips. Therefore, in this paper, we propose a method of calibration to estimate the positions of the accelerometers in an inertial sensor array.

Uncertainties in static parameters are estimated in a calibration procedure, so that they can later be compensated for. Such uncertainties for individual accelerometer triads include misalignment of the sensitivity axes, unknown scaling factors, and biases. A common method used to estimate these errors is to use the property that the norm of the sensed gravitational field must remain constant, irrespective of the accelerometer orientation [5]–[11]. To estimate the accelerometer positions in a sensor array, one possible method is to expose the sensor array to a known reference motion using external equipment [10]–[13]. Calibration of the accelerometer positions in a sensor array have been addressed using no reference motion [14], where a non-linear least-squares optimization problem is solved using an iterative graph optimization scheme to jointly estimate the motion, the orientations and the positions of the sensing elements. Their experiments yielded a mean position error of approximately $650\,\mu\mathrm{m}$. However, the computational complexity is cubic in the number of time samples. Further, the cost of calibration using external equipment often exceeds the cost of the sensor array, and the external equipment may not always be accessible.

In this study, we extend the work done in [4] to simultaneously estimate the positions of the accelerometers and the motion using measurements from an inertial measurement unit

This work was partially supported by the Wallenberg Autonomous Systems and Software Program (WASP), and by the Swedish Foundation for Strategic Research (SSF) via the project ASSEMBLE.

(IMU) sensor array under arbitrary motion. By applying an iterative block coordinate descent optimization scheme, the motion dynamics of the time-series is first estimated with a maximum likelihood (ML)-estimator [4], given an initial guess of the accelerometer positions. Secondly, the motion dynamics of the time-series are fixed and the accelerometer positions are re-estimated. Thus, no reference motion nor external equipment is necessary, and each iteration can be computed with linear complexity in the number of time samples. This enables on-the-fly calibration of the accelerometer positions in the inertial sensor array.

II. Problem Formulation

In this section, the problem of how to estimate the relative positions of the sensing elements of a set of accelerometer triads spatially distributed on a rigid body will be studied. It will be assumed that the body is equipped with at least one gyroscope triad.

A signal model for the accelerometer measurements can be constructed from the decomposition of the accelerations of a point-mass described in the constant coordinates of a rotating frame [15]. That is, the k:th accelerometer triad located at $\boldsymbol{r}^{(k)}$ will at time instant n measure the acceleration

$$\boldsymbol{y}_{a,n}^{(k)} = \boldsymbol{s}_n + \underbrace{\boldsymbol{\omega}_n \times (\boldsymbol{\omega}_n \times \boldsymbol{r}^{(k)})}_{\text{Centrifugal}} + \underbrace{\dot{\boldsymbol{\omega}}_n \times \boldsymbol{r}^{(k)}}_{\text{Euler}} + \boldsymbol{\epsilon}_a^{(k)}, \quad (1)$$

where $\boldsymbol{s}$, $\boldsymbol{\omega}$, $\dot{\boldsymbol{\omega}}$ denote the translational acceleration, angular velocity, and angular acceleration, respectively. Here, it is assumed that the three sensing elements of accelerometer triads are orthogonal and located at the same position $\boldsymbol{r}^{(k)}$. Further, $\boldsymbol{\epsilon}_a^{(k)}$ denotes the measurement error of the accelerometer triad k. The measurement error is assumed to be white and distributed as $\boldsymbol{\epsilon}_a^{(k)} \sim \mathcal{N}(0, \sigma_a^2 \boldsymbol{I}_3)$, i.e., the error is zero-mean Gaussian distributed with covariance $\sigma_a^2 \boldsymbol{I}_3$.

The angular velocity is equal for all points on a rigid body [15] and, thus, the measurements from the j:th gyroscope triad can be modeled as

$$\boldsymbol{y}_{g,n}^{(j)} = \boldsymbol{\omega}_n + \boldsymbol{\epsilon}_g^{(j)}, \quad (2)$$

where $\boldsymbol{\epsilon}_g^{(j)}$ denotes the measurement error of the j:th gyroscope triad. The measurement error of the gyroscope triads is also assumed to be white and Gaussian distributed as $\boldsymbol{\epsilon}_g^{(j)} \sim \mathcal{N}(0, \sigma_g^2 \boldsymbol{I}_3)$.

Concatenating the measurements from K accelerometer triads and G gyroscope triads, the full measurement vector at time n becomes

$$\boldsymbol{y}_n = \begin{bmatrix} \boldsymbol{y}_{a,n}^{(1:K)} \\ \boldsymbol{y}_{g,n}^{(1:G)} \end{bmatrix}.$$

Next, let $\boldsymbol{\theta} \stackrel{\text{def}}{=} \{\boldsymbol{r}^{(k)}\}_{k=1}^K$ denote the unknown positions of the accelerometers. Further, let

$$\boldsymbol{x}_n \stackrel{\text{def}}{=} \begin{bmatrix} \boldsymbol{\omega}_n^T & \dot{\boldsymbol{\omega}}_n^T & \boldsymbol{s}_n^T \end{bmatrix}^T$$

denote the unknown motion dynamics of the array for time sample n, and let $\boldsymbol{x}_{1:N}$ denote the motion dynamics from time sample 1 to N. Then the estimation of the positions of the accelerometers can be posed as the following ML-problem

$$\left\{\hat{\boldsymbol{x}}_{1:N}, \hat{\boldsymbol{\theta}}\right\} = \arg\max_{\boldsymbol{x}_{1:N}, \boldsymbol{\theta}} p(\boldsymbol{y}_{1:N}; \boldsymbol{x}_{1:N}, \boldsymbol{\theta}), \quad (3)$$

where $p(\cdot)$ is the probability density function of the observed measurement sequence $\boldsymbol{y}_{1:N}$. Only the relative positions of the accelerometer triads can be estimated, because (1) is independent of the choice of origin. Thus, the position of one accelerometer triad has to be selected as a reference position and, with out loss of generality, $\boldsymbol{r}^{(1)}$ is chosen as the reference position.

We assume that the measurements are independent in time, so that the ML-estimation problem in (3) is simplified to

$$\left\{\hat{\boldsymbol{x}}_{1:N}, \hat{\boldsymbol{\theta}}\right\} = \arg\max_{\boldsymbol{\theta}} \prod_{n=1}^{N} \max_{\boldsymbol{x}_n} p(\boldsymbol{y}_n; \boldsymbol{x}_n, \boldsymbol{\theta}). \quad (4)$$

That is, $\boldsymbol{x}_n$ is optimized to maximize the probability of observing the measurement $\boldsymbol{y}_n$ for all time samples, in conjunction with optimizing $\boldsymbol{\theta}$ to maximize the probability of observing all measurements $\boldsymbol{y}_{1:N}$.

An ML-estimator for the motion dynamics estimation,

$$\hat{\boldsymbol{x}}_n = \arg\max_{\boldsymbol{x}_n} p(\boldsymbol{y}_n; \boldsymbol{x}_n, \boldsymbol{\theta}), \quad (5)$$

has been proposed and evaluated in [4]. Its theoretical results show that an accuracy improvement can be obtained beyond that achieved by averaging the measurements. However, experimental results indicate that the estimation accuracy of $\boldsymbol{x}_n$ is reduced by uncertainties in the accelerometer positions, thus, they need to be calibrated, i.e., estimated and compensated for.

To seek a unique solution to problem in (4), certain identifiable conditions need to be fulfilled. For a fixed value of $\boldsymbol{\theta}$, the problem in (5) is observable if, and only if, there are at least one gyroscope triad and three accelerometer triads spanning a 2D space [4]. Hence, these are also necessary (but not sufficient) conditions for the ML-estimation problem in (4) to have a unique solution. Another necessary condition for the problem in (4) to be well defined can be found by looking at the number of unknown parameters and measurements that are available in a time series of length N. Since multiple gyroscope measurements do not provide any new information, there will be $3(K+1)N$ measurements and $3(K-1)+9N$ unknowns. Hence a necessary condition for (4) to have a unique solution is that $N \geq (K-1)/(K-2)$, which has a minimum $N \geq 2$.

Moreover, there will be a physical bound that limits the accuracy by which the positions of the sensing elements can be estimated. Capacitive MEMS accelerometers, which consist of a proof mass suspended on a mechanical frame by a spring, can be modeled as a second order system [16], where the resonant frequency ω_0 is typically much higher than the expected maximum frequency component of the acceleration signal. The mechanical displacement of the proof mass along the sensitivity axis is then

$$d = \frac{y_a}{\omega_0^2}, \quad (6)$$

where y_a is the measured acceleration, defined in (1). The resonance frequency of typical consumer-grade accelerometers are in the low-kilohertz range [1], yielding mechanical displacements in the range of tens of nanometres when exposed to the gravitational acceleration. The length scale of the mechanical displacement of the proof mass can be considered the limit for which the sensing element remains at constant position during sensing.

III. Proposed Solution

The optimization problem in (4) has a natural separation in the variables $\boldsymbol{x}_i$ and $\boldsymbol{\theta}$ and, thus, we propose solving the optimization problem with an alternating optimization scheme, also known as the block coordinate descent method [17]. In this method, one set of parameters are fixed at constant values while another set is being optimized, and then the reverse is performed, thus alternating between optimizing different blocks of the parameters.

For problem (3), $\boldsymbol{\theta}$ is first fixed to the value $\boldsymbol{\theta}^{\diamond}$ and then problem (5) is solved using the ML-estimator proposed in [4]. The obtained solution for the motion dynamic variables is then set to be fixed, i.e., $\boldsymbol{x}^{\diamond}_{1:N} = \hat{\boldsymbol{x}}_{1:N}$, and

$$\hat{\boldsymbol{\theta}} = \arg\max_{\boldsymbol{\theta}} p(\boldsymbol{y}_{1:N}; \boldsymbol{x}^{\diamond}_{1:N}, \boldsymbol{\theta}), \tag{7}$$

is solved. With the new estimation of $\hat{\boldsymbol{\theta}}$, the problem of estimating the motion dynamics in (5) is solved again. Alternating between these two methods yields an algorithm to find a solution to the original problem in (3).

To solve problem (7), it is recognized that (1) is linear in $\boldsymbol{r}^{(k)}$ given fixed values of $\boldsymbol{s}_n, \boldsymbol{\omega}_n, \dot{\boldsymbol{\omega}}_n$. That is, by formulating the cross product as a matrix multiplication of a skew-symmetric matrix, i.e., $\boldsymbol{\Omega_a b} = \boldsymbol{a} \times \boldsymbol{b}$, (1) can be reformulated as

$$\boldsymbol{y}^{(k)}_{a,n} = \boldsymbol{s}_n + \boldsymbol{A}_n \boldsymbol{r}^{(k)} + \boldsymbol{\epsilon}^{(k)}_g, \tag{8}$$

where $\boldsymbol{A}_n = \boldsymbol{\Omega}^2_{\omega_n} + \boldsymbol{\Omega}_{\dot{\omega}_n}$. Given the data from N time samples, the least square estimate of $\boldsymbol{r}^{(k)}$ is

$$\boldsymbol{r}^{(k)} = \left(\sum_{n=1}^{N} \boldsymbol{A}_n^T \boldsymbol{A}_n \right)^{-1} \left(\sum_{n=1}^{N} \boldsymbol{A}_n^T (\boldsymbol{y}^{(k)}_{a,n} - \boldsymbol{s}_n) \right). \tag{9}$$

For $\boldsymbol{r}^{(k)}$ to have a unique solution, the matrix $\begin{bmatrix} \boldsymbol{A}_1^T & \cdots & \boldsymbol{A}_N^T \end{bmatrix}^T$ must have full rank. A necessary condition for $\boldsymbol{A}_n$ to have full rank is that $\boldsymbol{\omega}_n$ and $\dot{\boldsymbol{\omega}}_n$ are not parallel (see Lemma 1 in the Appendix). Thus, $\boldsymbol{r}^{(k)}$ has an unique solution if the angular velocity vectors and the angular acceleration vectors not are mutually parallel for all time samples.

In summary, the calibration algorithm is shown as pseudo-code in Algorithm 1. Given a recorded measurement series $\boldsymbol{y}_{1:N}$ of N time samples, select a reference accelerometer position and make an initial guess of the other accelerometer positions, i.e., $\hat{\boldsymbol{r}}^{(2:K)}$. Then alternate between estimating $\hat{\boldsymbol{x}}_{1:N}$ and $\hat{\boldsymbol{r}}^{(2:K)}$. It is noteworthy that the inverse on line 10 only has to be calculated once for all K accelerometers. One iteration in the while loop is denoted as one iteration in the optimization.

Algorithm 1 Calibration of sensor array

1: $\boldsymbol{r}^{(1)} \leftarrow$ reference position
2: $\hat{\boldsymbol{r}}^{(2:K)} \leftarrow$ initial guess
3: $\boldsymbol{y}_{1:N} \leftarrow$ record N time samples
4: **while** not converged **do**
5: $\quad \hat{\boldsymbol{\theta}} \leftarrow \begin{bmatrix} \boldsymbol{r}^{(1)} & \hat{\boldsymbol{r}}^{(2:K)} \end{bmatrix}$
6: $\quad \hat{\boldsymbol{x}}_{1:N} \leftarrow \arg\max_{\boldsymbol{x}_{1:N}} p(\boldsymbol{y}_{1:N}; \boldsymbol{x}_{1:N}, \hat{\boldsymbol{\theta}})$
7: $\quad$ **for** $n = 1$ to N **do**
8: $\quad\quad \boldsymbol{A}_n \leftarrow \boldsymbol{\Omega}^2_{\hat{\boldsymbol{\omega}}_n} + \boldsymbol{\Omega}_{\hat{\dot{\boldsymbol{\omega}}}_n}$
9: $\quad$ **end for**
10: $\quad \boldsymbol{C} \leftarrow \left(\sum_{n=1}^{N} \boldsymbol{A}_n^T \boldsymbol{A}_n \right)^{-1}$
11: $\quad$ **for** $k = 2$ to K **do**
12: $\quad\quad \hat{\boldsymbol{r}}^{(k)} \leftarrow \boldsymbol{C} \left(\sum_{n=1}^{N} \boldsymbol{A}_n^T (\boldsymbol{y}^{(k)}_{a,n} - \hat{\boldsymbol{s}}_n) \right)$
13: $\quad$ **end for**
14: **end while**

Fulfilling the requirements for $\boldsymbol{r}^{(k)}$ to have an unique solution, it is possible to record a time-series of arbitrary motion and perform the accelerometer position calibration procedure without external calibration equipment. Another advantage is that the complexity of calculating the inverse of $\sum_{n=1}^{N} \boldsymbol{A}_n^T \boldsymbol{A}_n$ is constant and independent of the number of time samples. The computationally expensive operations are the summations on lines 10 and 12, which have linear computational complexity. Hence, the complete calibration algorithm has a complexity of $\mathcal{O}(N)$.

IV. Simulation

The ML-estimator for the motion dynamics, given a set of fixed accelerometer positions [4], has an accuracy that depends on the accuracy of the gyroscopes, the accuracy of the accelerometers, the geometry of the accelerometers, the number of IMUs, and the angular velocity. Thus, it is expected that the accuracy in estimating the accelerometer positions also depends on these quantities. Additionally, one can also expect the position accuracy to depend on the number of time samples in the recorded time series, as well as the angular acceleration, as they are included in (9).

The sensor array model considered in the simulation study is based upon the geometry of the real-world sensor array shown in Fig. 1 [18]. The array consists of 32 MPU9150 Invensense [19] inertial sensor chipsets located on the top and the underside of a printed circuit board (PCB). Each chipset contains an accelerometer triad, a gyroscope triad, and a magnetometer triad. A conceptual model of the sensor array is shown in Fig. 2. In the following simulations, it is assumed that the spatial separation is 6.3 mm in the xy-plane and 2 mm in the z direction. Further, the position error[1] is assumed to be normally distributed with a standard deviation of $\sigma_r = 1$ mm. The measurement errors of the accelerometers and the gyroscopes are assumed to be uncorrelated and to have

[1]The total error includes both the errors due to impressions in the mounting of the sensors on the PCB and the errors due to uncertainties in the location of the sensing elements within the IMU chips.

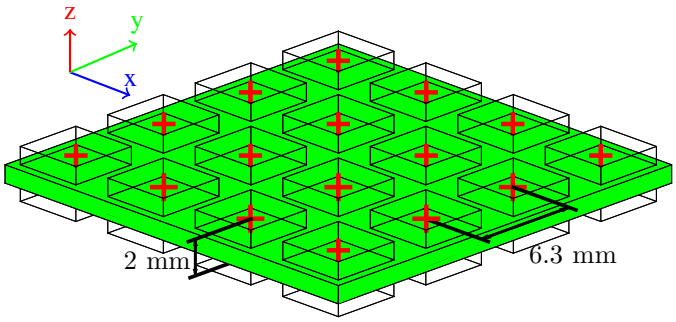

Fig. 2: The inertial sensor array considered in the simulations. 16 IMUs are located on the top and the underside of a PCB, respectively. The red crosses denote the position of the sensing elements inside the IMUs.

a standard deviation of $\sigma_a = 0.04\,\mathrm{m/s^2}$ and $\sigma_g = 0.06^\circ/\mathrm{s}$, respectively. Further, the gyroscopes are assumed to saturate at $\gamma_g = 2000^\circ/\mathrm{s}$. Although these specifications are for the MPU9150 Invensense, they reflect the typical performance of ultra-low-cost IMU.

To evaluate the accuracy of the accelerometer position estimator, a set of Monte Carlo simulations were conducted, each with 10^4 data realizations. In each realization, a random sequence of motion dynamics, $\boldsymbol{x}_{1:N}$, was generated where the directions of the linear acceleration, the angular velocity, and the angular acceleration vectors were sampled from the unit sphere. Since the translational acceleration enters the signal model in (8) linearly, the magnitude and direction of the translational acceleration will not affect the accuracy of the position estimates. The magnitude of the angular velocity and the angular acceleration, i.e., $||\boldsymbol{\omega}||$ and $||\dot{\boldsymbol{\omega}}||$, were either varied or held constant depending on the simulation settings.

For the considered array, it is useful to investigate what level of position accuracy is needed to reduce the estimation error of the angular velocity below that obtained by simply averaging the gyroscope measurements. Shown in Fig. 3 is the root-mean-square error (RMSE) of the angular velocity for different angular speeds. As can be seen, an accelerometer position error with a standard deviation of $\sigma_r = 10^{-4}\,\mathrm{m}$ can explain the measured error seen in the experiments presented in [4]. To obtain an estimation error which would be comparable to the accuracy obtained by averaging the gyroscope measurements, a position accuracy of $\sigma_r = 10^{-5}\,\mathrm{m}$ is needed. For the considered range of angular velocities, an error of $\sigma_r = 10^{-6}\,\mathrm{m}$ would be comparable to having no error at all.

In Fig. 4, the dependence of the number of time samples and the number of optimization iterations on the RMSE is shown for a high-dynamic motion trajectory. Here, the RMSE is calculated by averaging the error over all accelerometer position components, excluding the reference position. It is noteworthy that for two time samples, the RMSE of the accelerometer positions does not decrease with an increasing number of optimization iterations, indicating that additional conditions need to be fulfilled for the calibration problem in (4) to be well

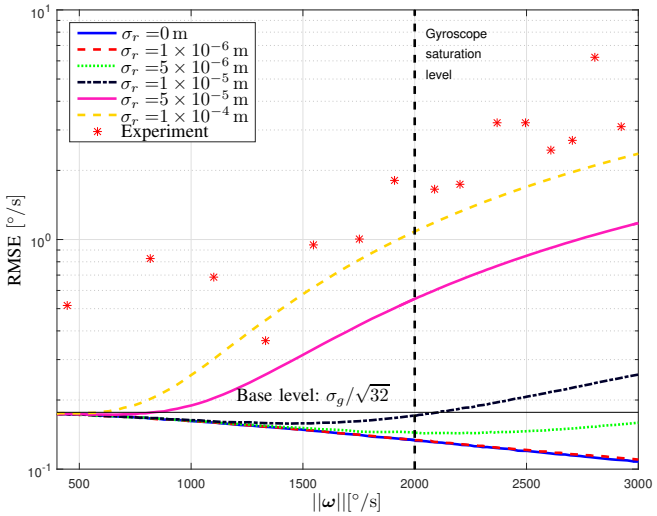

Fig. 3: The RMSE of the estimated angular velocity as a function of the magnitude of the true angular velocity and different levels of accelerometer position errors.

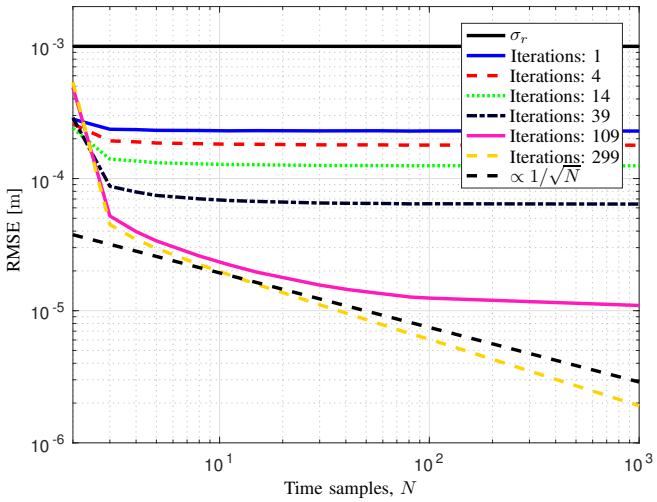

Fig. 4: The RMSE of the accelerometer position estimates for different number of time samples and optimization iterations. The magnitude of the angular velocity and angular acceleration were set to $||\boldsymbol{\omega}|| = 2000^\circ/\mathrm{s}$ (just below gyroscope saturation level) and $||\dot{\boldsymbol{\omega}}|| = 2000^\circ/\mathrm{s}^2$, respectively.

posed. However, with more than two time samples, the RMSE decreases with an increasing number of optimization iterations and time samples. For a sufficient number of iterations and more than two time samples, it is noticed that the RMSE of the accelerometer positions decreases with the inverse square-root of the number of time samples in the recorded series. That is, the RMSE is proportional to $N^{-1/2}$. This can be attributed to the linear estimator of the accelerometer positions in (9), the additive white noise on the positions, and by assuming that the estimation of the motion dynamics, $\hat{\boldsymbol{x}}_{1:N}$, have achieved their lower bound. All together, this would yield that the variance of $\hat{\boldsymbol{r}}^{(2:K)}$ should decrease as N^{-1} [20].

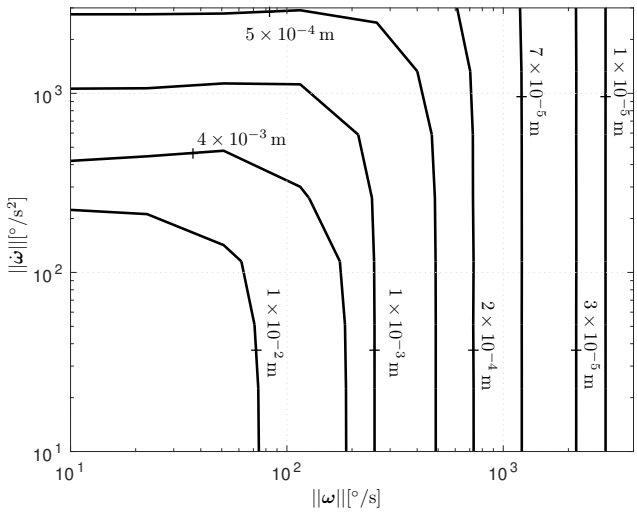

Fig. 5: The RMSE of the accelerometer position estimates for different magnitudes of angular velocity and angular acceleration. The number of time samples and optimization iterations were set to $N = 10$ and 200, respectively.

Furthermore, it is of interest to see how the dynamics of the motion affects the accuracy of the accelerometer positions estimation. Shown in Fig. 5 is the dependence on the magnitude of the angular velocity and the magnitude of the angular acceleration. As can be seen, the higher the magnitude of the angular acceleration and the angular velocity, the more the accelerometer position error decreases.

V. Conclusions

A maximum likelihood estimator has been proposed for estimating the positions of the accelerometers in an inertial sensor array. Using an iterative block coordinate descent scheme, the method simultaneously estimates the positions of the accelerometers and the motion dynamics of the inertial sensor array. Consequently, the calibration method does not require a predefined motion sequence nor any external equipment to estimate the accelerometers positions. Further, the calibration problem can be solved with a complexity which is linear in the number of time samples, which enables on-the-fly calibration. As long as the motion used for the calibration has sufficient dynamics, the accelerometer positions can be estimated to an accuracy that renders the sensor fusion algorithm in [4] reliable.

Furthermore, simulations indicate that, given sufficient optimization iterations, the variance of the accelerometer positions decreases with the inverse of the number of time samples in the recorded series. This suggests that the estimator approaches the lower bound of estimating the motion of the same recorded series.

Further, the results (given the considered array of 32 IMUs) indicate that an acceleration position accuracy worse than $10\,\mu\mathrm{m}$ will render the angular acceleration estimation from only the accelerometers worse than average from the equivalent amount of gyroscopes. In the case of the high motion dynamics in Fig. 4, the measured acceleration can range between $2 - 3g$. Given that the resonance frequency of typical consumer-grade accelerometers is in the low-kilohertz range [1], i.e., approximately $5\,\mathrm{kHz}$, the maximum displacement of the sensing element is approximately $30\,\mathrm{nm}$. That is, given the 32 IMU array, an accelerometer position accuracy of $1\,\mu\mathrm{m}$ is approximately a factor 30 bigger than the maximum mechanical displacement, so the position of the proof-mass in the considered length-scale can be considered constant during sensing. That is, the design of a capacitive MEMS accelerometer is not likely to impede the accelerometer position estimation. Further, an accelerometer position accuracy in the order of $1\,\mu\mathrm{m}$ was obtained from the simulations of the calibration method using the motion dynamics in Fig. 4 and 1000 time samples. Consequently, errors in the position of the accelerometers can thus be compensated for, to such a level that render the motion estimation in [4] reliable.

Moreover, future work could be to investigate how the distance separation of the accelerometers influence the accuracy of the accelerometer position estimation, given that estimation of the angular velocity depends on it. Also, the task of deriving the Cramér bound for the calibration problem remains, and investigate whether the alternating optimization method is statistically efficient. Other open questions relate to the necessary and sufficient conditions that must be fulfilled for the proposed calibration method to work, as well as the theoretical aspects of convergence in the optimization loop.

Appendix

Lemma 1. *If $\boldsymbol{A}, \boldsymbol{B} \in \mathbb{R}^{3,3}$ are non-zero skew-symmetric matrices and $k\boldsymbol{A} = \boldsymbol{B}$ for a constant k, then the rank of $\boldsymbol{A}^2 + \boldsymbol{B}$ is 2.*

Proof. The eigenvalues of real non-zero skew-symmetric matrices are purely imaginary and are paired in complex conjugates. Thus, the eigenvalues of $\boldsymbol{A}$ are $\{\lambda i, -\lambda i, 0\}$, and the eigenvalues of $\boldsymbol{A}^2 + \boldsymbol{B}$ are $\{-\lambda^2 + k\lambda i, -\lambda^2 - k\lambda i, 0\}$. Consequently, the rank of $\boldsymbol{A}^2 + \boldsymbol{B}$ is 2. □

References

[1] D. K. Shaeffer, "MEMS inertial sensors: A tutorial overview," *IEEE Communications Magazine*, vol. 51, no. 4, pp. 100–109, April 2013.

[2] J. O. Nilsson and I. Skog, "Inertial sensor arrays - a literature review," in *2016 European Navigation Conference (ENC)*, May 2016, pp. 1–10.

[3] N. El-Sheimy and X. Niu, "The Promise of MEMS to the Navigation Community," *InsideGNSS*, pp. 6+, Apr 2007.

[4] I. Skog, J.-O. Nilsson, P. Händel, and A. Nehorai, "Inertial Sensor Arrays, Maximum Likelihood, and Cramér-Rao Bound," *IEEE Transactions on Signal Processing*, vol. 64, no. 16, pp. 4218–4227, Aug 2016.

[5] I. Skog and P. Händel, "Calibration of a MEMS inertial measurement unit," in *in Proc. XVII IMEKO WORLD CONGRESS, (Rio de Janeiro*, 2006.

[6] M. Glueck, D. Oshinubi, P. Schopp, and Y. Manoli, "Real-time autocalibration of MEMS accelerometers," *IEEE Transactions on Instrumentation and Measurement*, vol. 63, no. 1, pp. 96–105, Jan 2014.

[7] J. O. Nilsson, I. Skog, and P. Händel, "Aligning the forces - eliminating the misalignments in IMU arrays," *IEEE Transactions on Instrumentation and Measurement*, vol. 63, no. 10, pp. 2498–2500, Oct 2014.

[8] C.-W. Tan and S. Park, "Design of accelerometer-based inertial navigation systems," *IEEE Transactions on Instrumentation and Measurement*, vol. 54, no. 6, pp. 2520–2530, Dec 2005.

[9] K. Parsa, T. A. Lasky, and B. Ravani, "Design and implementation of a mechatronic, all-accelerometer inertial measurement unit," *IEEE/ASME Transactions on Mechatronics*, vol. 12, no. 6, pp. 640–650, Dec 2007.
[10] S. Park, C.-W. Tan, and J. Park, "A scheme for improving the performance of a gyroscope-free inertial measurement unit," *Sensors and Actuators A: Physical*, vol. 121, no. 2, pp. 410 – 420, 2005.
[11] D. Dubé and P. Cardou, "The calibration of an array of accelerometers," *Transactions of the Canadian Society for Mechanical Engineering*, vol. 35, no. 2, p. 251, 2011.
[12] P. Cappa, F. Patane, and S. Rossi, "Two calibration procedures for a gyroscope-free inertial measurement system based on a double-pendulum apparatus," *Measurement Science and Technology*, vol. 19, no. 5, p. 055204, 2008.
[13] P. Schopp, L. Klingbeil, C. Peters, A. Buhmann, and Y. Manoli, "Sensor fusion algorithm and calibration for a gyroscope-free IMU," *Procedia Chemistry*, vol. 1, no. 1, pp. 1323 – 1326, 2009.
[14] P. Schopp, H. Graf, W. Burgard, and Y. Manoli, "Self-calibration of accelerometer arrays," *IEEE Transactions on Instrumentation and Measurement*, vol. 65, no. 8, pp. 1913–1925, Aug 2016.
[15] L. Landau and E. Lifshitz, *Mechanics*, 3rd ed., ser. 10. Butterworth-Heinemann, 1976, no. volume 1.
[16] S. D. Senturia, *A Capacitive Accelerometer*. Boston, MA: Springer US, 2001, pp. 497–530.
[17] P. Tseng, "Convergence of a block coordinate descent method for nondifferentiable minimization," *Journal of Optimization Theory and Applications*, vol. 109, no. 3, pp. 475–494, 2001.
[18] I. Skog, J. O. Nilsson, and P. Händel, "An open-source multi inertial measurement unit (MIMU) platform," in *2014 International Symposium on Inertial Sensors and Systems (ISISS)*, Feb 2014, pp. 1–4.
[19] *MPU-9150 Product Specification*, InvenSense Inc., 8 2013, rev. 4.3.
[20] S. M. Kay, *Fundamentals of Statistical Signal Processing: Estimation Theory*. Upper Saddle River, NJ, USA: Prentice-Hall, Inc., 1993.